# Separation of Adsorption and Surface Reaction Rates: Dynamic Studies in a Catalytic Slurry Reactor

Dynamic experiments provide an opportunity to determine, separately, values of the adsorption and surface reaction rates occurring in a heterogeneous, catalytic reaction. In this method it is not necessary to assume that either adsorption, surface reaction, or desorption controls the rate, in contrast to the procedure used for analyzing steady state rate data.

The dynamic method is applied to experimental data for the oxidation of sulfur dioxide in a three-phase aqueous-slurry reactor using activated carbon as the catalyst. The results for 274.5 K show that both rates of reversible adsorption of oxygen and the subsequent, irreversible surface reaction affect the overall rate. Neither process can be considered to be controlling.

The data required for the analysis are the zero and first moments of the response in the effluent gas to a disturbance in the feed, the adsorption equilibrium constant for oxygen, and appropriate mass transfer coefficients.

**BUM-JONG AHN,**
**B. J. McCOY, and**
**J. M. SMITH**

**University of California**
**Davis, CA 95616**

## SCOPE

The usual procedure—the Hougen and Watson (1947) method—for analyzing steady state rate data for heterogeneous, catalytic reactions is to assume one process to be controlling in the sequence of adsorption, surface reaction, and desorption. Without this assumption the analytical expressions for the rate become too cumbersome to use. Perhaps more important, steady state data cannot provide information about the magnitudes of rates of the individual processes.

When one process is assumed to be slow, the others occur at near equilibrium. Then the rate equation formulated by the Hougen and Watson method includes equilibrium constants for these processes. Hence, an indirect way to test the assumption of a single processs controlling the overall rate is to compare separately determined equilibrium constants, for example for adsorption, with the values for these constants that must be used in the Hougen and Watson equation to correlate the rate data. Most such comparisons have been unsuccessful, leading to the conclusion that the so-called equilibrium constants in the Hougen and Watson equations are best regarded as empirical constants. However, Kabel and Johanson (1962) and Raghavan and Doraiswamy (1977) have found satisfactory agreement between adsorption equilibrium constants determined separately and by correlating steady state rate data.

As pointed out by Bennett (1967, 1976), dynamic experiments provide an opportunity to avoid the controlling-process assumption, since adsorption, surface reaction, and desorption can occur at different rates during the transient period. During this period adsorbed concentrations as well as fluid-phase values are changing with time. At steady state, such concentrations are constant and the rates of adsorption, surface reaction, and desorption are identical.

Our objective was to develop the dynamic method for a slurry reactor and use it with experimental data to determine reaction rates for the individual processes. Solution of the equations describing reaction under dynamic conditions in the real time domain is difficult. However, solutions in the Laplace domain are relatively simple and lead to tractable expressions for the moments. These moment equations include separate rate constants for the several processes that together comprise the overall reaction.

To use the Laplace approach, the system must be linear. The oxidation of sulfur dioxide in an aqueous slurry of activated carbon particles meets this requirement. Komiyama and Smith (1975) found that with an excess of sulfur dioxide the reaction was first-order in oxygen and zero-order in sulfur dioxide. The reaction is irreversible at low temperatures, and the rate is unaffected by the sulfur trioxide produced as long as the sulfuric acid concentration in the water is low. Dynamic experiments were carried out with this system at 274.5 K by introducing a step function of sulfur dioxide and oxygen in the gas feed to the slurry reactor and analyzing the effluent gas for the oxygen concentration.

The zero and first moments of the oxygen response curve provide two relations between the adsorption and surface reaction rate constants. The adsorption of oxygen on activated carbon is reversible. Also, mass transfer processes are involved in the slurry reactor. Hence, the adsorption equilibrium constant for oxygen and some mass transfer coefficients are needed before the values for the two moments can be used to determine the adsorption and surface reaction rate constants. The necessary mass transfer coefficients in our slurry reactor were available from previous studies and the adsorption equilibrium constant was measured independently with dynamic adsorption experiments. The gas concentration inside the bubbles could be described with either a plug-flow or well-mixed model with very little effect on the determined values of rate constants.

## CONCLUSIONS AND SIGNIFICANCE

**A method that utilizes dynamic rate data has been developed for obtaining individual values of adsorption and surface reaction rate constants for a heterogeneous, catalytic reaction. The method is illustrated with data for the oxidation of sulfur dioxide in slurries of activated carbon at 274.5 K. Zero and first moments in the effluent gas were measured in response to a step-concentration change in the feed gas. The results show that neither adsorption or surface reaction controls the overall, intrinsic rate. Average values of the desorption rate constant, $k_a/K = 0.02\ s^{-1}$, and surface reaction rate $k_r = 0.012\ s^{-1}$, suggest that for every three molecules of oxygen reversibly adsorbed on the catalyst, two are desorbed and one reacts. Both adsorption and surface reaction affect the overall rate. The rate constant, $k_a$, for adsorption of oxygen agrees with the earlier results of Niiyama and Smith (1977) who studied rates of oxygen adsorption in the absence of sulfur dioxide.**

**To obtain separate values of $k_a$ and $k_r$, it is necessary to know the adsorption equilibrium constant $K$. We used a value, at 274.5 K, obtained from independent oxygen adsorption data. This introduces some uncertainty since the presence of sulfur dioxide may influence oxygen adsorption capacity. Since oxygen solubility in water is very low, the effect of reaction conditions on $K$ may be small. In principle, $K$ under reaction conditions could be found from second moments. However, the accuracy of experimental second moments is much less than that for first and zero moments. More information would be helpful on the relation between adsorption equilibrium constants in reactive and nonreactive systems.**

**It is shown that analysis of zero moments gives the mass transfer coefficient from gas bubble to liquid as well as a relation between $k_a$ and $k_r$. In addition, the mass transfer coefficient, $k_s$, from liquid to outer surface of the particles and the intraparticle diffusivity $D_e$ are needed before $k_a$ and $k_r$ can be obtained from the zero and first moments. Because the carbon particles were very small, results for $k_a$ and $k_r$ are not sensitive to $k_s$ and $D_e$. Hence, values previously available (Niiyama and Smith, 1977; Furusawa and Smith, 1973) could be used without introducing significant errors.**

**Experimentally measured first moments include the residence time in the "dead" volumes of the apparatus. Correction for such residence times can introduce errors, especially when the dead volume is large with respect to the volume of the reactor, in our case the volume of the slurry itself. This problem was circumvented by relating the measured first moment to a modified zero moment.**

**This study demonstrates the value of dynamic studies for providing quantitative information about the rates of the adsorption and surface reaction processes that occur in heterogeneous catalytic reactions. The method is not limited to slurry reactors and should be applicable to any reactor type as long as the rate processes involved are all first-order.**

## INTRODUCTION

The usual procedure for developing rate equations for heterogeneous catalytic reactions is that originally developed by Hougen and Watson (1947). In this method, based upon the concepts of Langmuir (1921) and Hinshelwood (1940), a series of adsorption, surface reaction, and desorption processes are proposed to represent the mechanism of the reaction. The key assumption is then made that one of the processes is slow enough to control the rate of the overall reaction. The validity of this assumption is difficult to evaluate from steady state rate data, because the equations involve combinations of rate and equilibrium (for the steps presumed to be fast) constants. Often there are a sufficient number of these constants that steady state rates can be adequately predicted by more than one equation, each arising from a different assumption.

Auxiliary measurements in a few cases have been useful in ascertaining the controlling process. Kabel and Johanson (1962) correlated data for the rate of dehydration of ethanol, using a cation exchange resin as catalyst, in terms of an equation based upon surface reaction controlling the overall rate. This expression involved equilibrium constants for adsorption steps. Independent adsorption measurements in the absence of reaction gave values for these equilibrium constants that agreed with those in the rate equations. Raghavan and Doraiswamy (1977), in studies of the isomerization of n-butene, also found agreement between the adsorption equilibrium constant for n-butene determined independently and that in the rate equation formulated by the Hougen and Watson method. However, these two examples seem to be exceptions to the normal situation where separate equilibrium measurements cannot be used to evaluate the adsorption equilibrium constants in the rate equation. The general conclusion has been that such quantities in the rate equation are best considered as arbitrary constants. More detailed discussions of the limitations of the Hougen and Watson procedure are available in review papers (Weller, 1975; Smith, 1982).

Perhaps a more serious problem with assuming that one step controls the rate is that it is then impossible to evaluate and compare separate values for the rates of adsorption, surface reaction, and desorption. As pointed out by Bennett (1967, 1976), Kobayashi and Kobayashi (1972), and Suzuki and Smith (1971), dynamic measurements offer the possibility of avoiding the assumption of a controlling step. In dynamic experiments the adsorbed concentrations (surface coverage) change with time. Then the net rate of adsorption is not equal to the rate of surface reaction—unlike the situation at steady state. The result is that dynamic experiments can, in principle, be used to evaluate adsorption and surface rate constants separately.

The governing differential equations describing dynamic behavior are not easily solved in the real-time domain. Also, the curve-fitting procedure necessary for evaluating parameters in the required numerical solution does not always lead to accurate results. However, if the governing equations are linear, it is straightforward to obtain a solution in the Laplace domain and thus to generate moments. The moment equations so obtained are simply related to the transport, adsorption, and surface reaction rate parameters that describe the experimental situation.

A reaction system that conforms to the linear limitation is the catalytic oxidation of sulfur dioxide in aqueous slurries of activated carbon. Komiyama and Smith (1975) found from steady state measurements that the reaction, at atmospheric pressure and ambient temperature, was first-order in oxygen and zero-order in sulfur dioxide (above gas concentrations of 0.3%). The very low solubility of oxygen in water is consistent with first-order reaction. The mathematical treatment is based upon reversible adsorption of oxygen and an irreversible surface reaction. Reversible adsorption was achieved experimentally by pretreating the activated carbon with oxygen to occupy irreversible sites. Both our experiments (Figure 2) and those of Mattson and Mark (1971) show that irreversible adsorption can occur. The reaction itself was essentially irreversible because of the large reaction equilibrium constant at room temperature. Desorption of the adsorbed sulfur trioxide product was assumed to be rapid since $SO_3$ is highly soluble in water.

The experiments were carried out by introducing a step function of a gaseous mixture of $SO_2$, $O_2$, and helium into a slurry that was

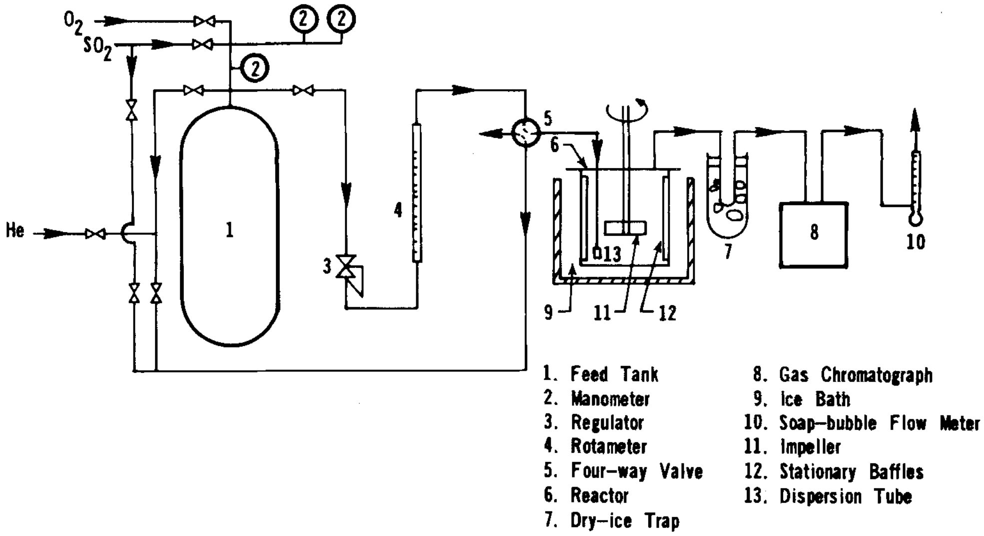

**Figure 1. Diagram of apparatus.**

properly pretreated with oxygen and sulfur dioxide. Then the oxygen concentration in the effluent gas was measured as a function of time. From the response curves obtained from these measurements the zero and first moments were calculated for runs at various gas flow rates and catalyst concentrations.

The theoretical expression for the first moment contains the ratio of the adsorption and surface reaction rate constants, $k_a$ and $k_r$. The zero moment equation provides a second relationship, which is the combination of rate constants that describe the overall, intrinsic kinetics. Hence, experimental values of these two moments are sufficient to evaluate, separately, the individual rate constants and determine the contribution of adsorption and of surface reaction to the overall rate. The zero moment provides the information obtainable from steady state data while the first moment provides the additional dynamic information that permits separate evaluation of the rate constants.

In addition to the moments, it is necessary to know mass transport coefficients of oxygen from gas-to-liquid, $k_L$, and liquid-to-particle, $k_s$, and also the intraparticle diffusivity, $D_e$, of oxygen in the liquid-filled pores of the carbon. Further, the individual rate constants are combined with the equilibrium constant $K$, which describes the reversible adsorption of oxygen. Hence, to evaluate $k_a$ and $k_r$ separately, $K$ must be known. These quantities were determined in part from our data and in part from Niiyama and Smith (1977), who studied rates and equilibrium for the adsorption of oxygen in aqueous slurries of the same carbon. Higher moments would provide additional relations between the rate constants, but the accuracy of experimental values for higher moments is questionable.

## EXPERIMENTAL

Figure 1 is a schematic drawing of the slurry reactor and auxiliary apparatus. The Pyrex reactor, about 0.15 m high and 0.1 m in diameter, was equipped with an eight-bladed, Teflon impeller. The impeller was located about 0.050 m from the bottom of the reactor and operated with a variable-speed motor. In addition, a stainless steel insert containing eight stationary baffles was placed along the inside wall of the Pyrex cylinder. DeWaal and Okeson (1966) found no difference between glass and stainless steel reactors for the rate of oxidation of aqueous sulfite solutions. However, copper is a catalyst for such oxidations, so brass apparatus cannot be used. The detailed dimensions and location of the impeller and baffles are the same as employed by Furusawa and Smith (1973) and Niiyama and Smith (1976, 1977). Hence the energy dissipation rate is known for the impeller speed used (16 rps); in addition, the mass transfer coefficients, from particle to liquid, found in these earlier studies should be applicable.

The feed gas, prepared in the feed tank to be of constant composition (10% $O_2$, 1% $SO_2$ and 89% He), was introduced through a fritted glass dispersion tube (13) 0.012 m dia. × 0.021 m long, located near the bottom of the reactor. The whole reactor assembly was immersed in a bath through which cold water was recirculated. All data were obtained at the low temperature of 274.5 K to increase the effect on the moment values of adsorption and reaction with respect to mass transport processes.

TABLE 1. PROPERTIES OF ACTIVATED CARBON*

| | |
|---|---|
| Surface area ($N_2$, BET method) | 1.05 ~ 1.15 $km^2/kg$ |
| Solid density | 2.1 × $10^3$ $kg/m^3$ |
| Particle density, $\rho_p$ | 0.85 × $10^3$ $kg/m^3$ |
| Porosity, $\beta$ | 0.60 |
| Avg. particle diameter (150–250 mesh) | 82.5 $\mu m$ |
| Mean pore radius in particles | 1.3 nm |

* From data sheet, type BPL activated carbon, Calgon Corp.

A four-way valve (5) was used to introduce a step function of the feed gas mixture. The effluent gas flowed through a dry ice-alcohol trap (7). The removal of water in the trap greatly reduced the analysis time between consecutive samples. A Varian gas chromatograph, model 1400, (8), with a 2 ft. (0.6 m) column of Porapak R, operated at 423 K, was used to analyze effluent gas samples for oxygen. The total volume, measured by water displacement, of the reactor, tubing, and trap between the four-way valve and the sample injection valve of the chromatograph was 1.32 × $10^{-3}$ $m^3$.

Type BPL activated carbon, a bituminous-coal based material, was used as a catalyst. The particle size was 82 $\mu m$, the average size of particles retained between 150- and 250-mesh screens. The carbon was dried overnight at 390 K, then weighed and boiled in distilled water for more than four hours prior to being added to the reactor. The small particle size caused the effect of intraparticle diffusion on the results to be negligible. The mass of carbon in the slurry was chosen to be relatively large. This gave relatively long and hence more accurate first moments. The mass was not so large as to prevent a uniform slurry or a settling of particles.

Properties of the carbon and operating conditions for the experiments are summarized in Tables 1 and 2.

### Operating Procedure

The slurry, in place in the reactor, was purged for two hours with helium. Next the slurry was pretreated with oxygen in a 10% $O_2$, 90% helium stream, followed by oxygen adsorption runs, and finally pretreated with

TABLE 2. OPERATING CONDITIONS

| | |
|---|---|
| Reactor vol., incl. tubing and trap | 1.32 × $10^{-3}$ $m^3$ |
| Feed gas composition | |
| For $O_2$ adsorption runs | 10% $O_2$ and 90% He |
| For reaction runs | 10% $O_2$, 1% $SO_2$, and 89% He |
| Gas flow rate | 1.7 × $10^{-6}$ to 1.06 × $10^{-5}$ $m^3/s$ |
| Impeller speed | 16 rev/s |
| Temperature | 274.5 ± 1 K |
| Pressure | Atmospheric |
| Mass conc. of carbon in slurry, $m_s$ | 0.143 and 0.209 × $10^3$ $kg/m^3$ |

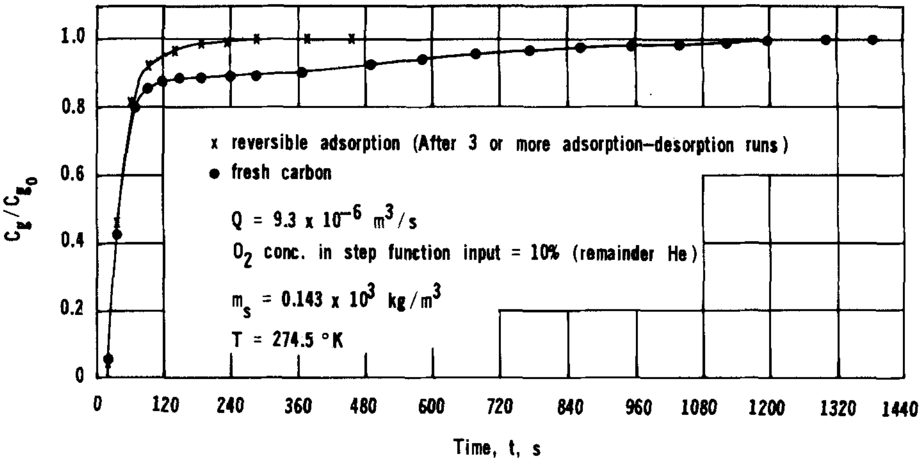

Figure 2. Response curve for oxygen adsorption.

sulfur dioxide. Then reaction runs were made. The purpose of oxygen pretreatment was to eliminate especially active sites on which oxygen would be irreversibly adsorbed. The adsorption runs were made to determine the adsorption equilibrium constant, $K$, for oxygen on the remaining reversible sites at the operating temperature. The procedure employed to measure $K$ is the same as that described by Niiyama and Smith (1976).

Figure 2 demonstrates irreversible oxygen adsorption for fresh carbon. The lower response curve is for fresh carbon and the other for carbon that had twice been subjected to oxygen pretreatment. No further change in response curves was observed after the third run, suggesting that the area above and to the left of the upper curve in Figure 2 is proportional to the amount of reversible adsorption. The area between the two curves is proportional to the amount of irreversibly adsorbed oxygen. The plateau in the curve for fresh carbon is similar to that expected for an irreversible reaction between oxygen and adsorbed species. Hence, the difference between the two curves could also be explained at least in part by reaction of oxygen with adsorbed species.

The purpose of the pretreatment with sulfur dioxide was to have sufficient adsorbed $SO_2$ to ensure a zero-order rate dependency, even during the initial period of the subsequent reaction run. Thus, the slurry was pretreated with a 20% $SO_2$–80% He mixture at 274.5 K for one-half hour at a gas flow rate of about $7 \times 10^{-6}$ m$^3$/s (298 K, 101 kPA). This was followed by a helium purge of about one-half hour to remove excess sulfur dioxide dissolved in the water.

The runs were made with a height of slurry of about 0.136 m to minimize the dead volume due to the space above the liquid level in the reactor. Gas flow rates were measured accurately with a soap-bubble flowmeter (10 in Figure 1). The data in all cases consisted of response curves drawn through discrete data points, as illustrated in Figures 2 and 3.

## THEORY OF DYNAMIC ADSORPTION AND REACTION

The derivation of moment equations for the dynamic behavior of three-phase slurry systems has been presented by Ramachandran and Smith (1977) and by Weng and Smith (1984). In the former work the accumulation term in the gas bubbles was neglected. The argument for this assumption is based upon the small residence time of the bubbles in the slurry and probably is valid in most cases. However, the more general equations developed in the second paper are employed with our data.

### Basic Equations

The more important restrictions in the derivation are: (1) plug flow of discrete gas bubbles (this assumption does not significantly affect our results, as seen later); (2) uniform catalyst-particle and liquid concentrations throughout the slurry; and (3) first-order and reversible adsorption of oxygen, and first-order and irreversible surface reaction on the carbon sites. Then the four mass-conservation equations for oxygen in the gas bubbles, in the slurry liquid, in the liquid-filled pores of the carbon particles, and at a reaction site are:

$$V_B \frac{\partial C_g}{\partial t} = -v_B V_B \frac{\partial C_g}{dz} - k_L a_B (C_g/H - C_L) = 0 \qquad (1)$$

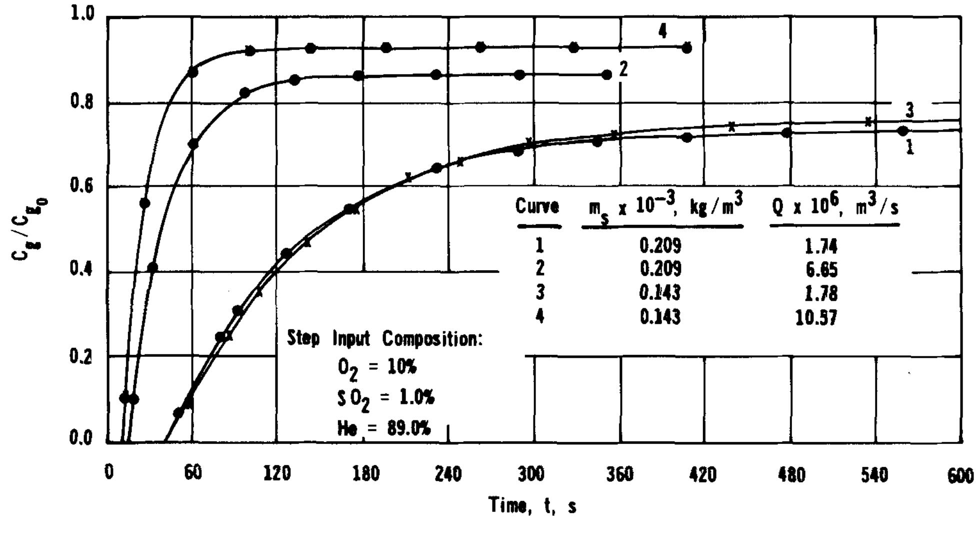

Figure 3. Response curves for reaction.

$$\left(1 - \frac{\beta m_s}{\rho_p}\right)\frac{dC_L}{dt} = \frac{k_L a_B}{L}\int_0^L (C_g/H - C_L)dz - k_s a_s[C_L - (C_i)_{r=R}] \quad (2)$$

$$\beta\frac{\partial C_i}{\partial t} = D_e\frac{1}{r^2}\frac{\partial}{\partial r}\left(r^2\frac{\partial C_i}{\partial r}\right) - \rho_p k_a(C_i - n/K) \quad (3)$$

$$\frac{dn}{dt} = k_a(C_i - n/K) - k_r n \quad (4)$$

It is Eq. 4 for reversible adsorption and irreversible surface reaction that applies in its complete form for dynamic studies and makes it possible to evaluate $k_a$ and $k_r$ separately.

The initial and boundary conditions are

$$C_g = C_{g_o} \text{ for } t \geq 0 \text{ at } z = 0 \quad (5)$$

$$C_L = C_i = n = 0 \text{ for } t = 0 \quad (6)$$

$$\left(\frac{\partial C_i}{\partial r}\right)_{r=0} = 0 \text{ for all } t \text{ and } z \quad (7)$$

$$k_s[C_L - (C_i)_{r=R}] = D_e\left(\frac{\partial C_i}{\partial r}\right)_{r=R} \text{ for all } t \text{ and } z \quad (8)$$

By solving these equations in the Laplace domain, and taking the limit of $\overline{C}_g$ and $d\overline{C}_g/ds$ as the Laplace variable $s$ approaches zero, the expressions for the zero and first moments are:

$$m_o = \exp(-K_L) + \frac{1 - \exp(-K_L)}{1 + \dfrac{K_L B_o}{1 - \exp(-K_L)}} \quad (9)$$

$$m_1 = \tau_g\left[1 - \frac{2}{1 + \dfrac{K_L B_o}{1 - \exp(-K_L)}}\right]\exp(-K_L) + \frac{\tau_g[1 + \exp(-K_L) + 2B_o] + K_L(B_s + \epsilon)}{\left[1 + \dfrac{K_L B_o}{1 - \exp(-K_L)}\right]^2} \quad (10)$$

The dimensional groups are defined as

$$B_s = \frac{Ra_s}{2k_L a_B}\left[\frac{\rho_p K}{\left(1 + \dfrac{k_r}{k_a/K}\right)^2} + \beta\right]\frac{\coth\phi_o - \phi_o\,\mathrm{csch}^2\phi_o}{\phi_o\left(1 + \dfrac{\phi_o\coth\phi_o - 1}{Bi}\right)^2} \quad (11)$$

$$\epsilon = \left(1 - \frac{m_s\beta}{\rho_p}\right)\Big/ k_L a_B \quad (12)$$

$$\tau_g = \frac{L}{v_B} = V_B V_L/Q \quad (13)$$

The dimensionless groups are:

$$B_o = \frac{k_s a_s}{k_L a_B}\left(1 - \frac{Bi}{Bi + \phi_o\coth\phi_o - 1}\right) \quad (14)$$

$$\phi_0^2 = \frac{\rho_p R^2}{D_e}\left[\frac{1}{K}\left(\frac{1}{k_a/K} + \frac{1}{k_r}\right)\right]^{-1} \quad (15)$$

$$K_L = \frac{k_L a_B L}{H v_B V_B} \quad (16)$$

$$Bi = Rk_s/D_e \quad (17)$$

The moments can be evaluated from the measured response curves, for a step-function input, from the equations

$$\left.\begin{aligned} m_o &= C_{g,\infty}/C_{g,o} \\ m_1 &= \int_0^\infty (C_{g,\infty} - C_g)/C_{g,o}\,dt \end{aligned}\right\} \quad (18)$$

### Modified Equations for Evaluating Rate Constants

Equation 9 for the zero moment can be rearranged to the form:

$$\frac{1}{1 - m_o} = \frac{1}{K_L B_o} + \frac{1}{1 - \exp(-K_L)} \quad (19)$$

For spherical particles, the outer surface area of the particles per unit volume of liquid, is given by

$$a_s = \frac{3m_s}{R\rho_p} \quad (20)$$

Next, Eq. 20 for $a_s$ and the second equality of Eq. 13 can be used to express $v_B$ in terms of $V_L$. Then the expressions for $B_o$ (Eq. 14) and $K_L$ (Eq. 16) can be simplified and substituted in Eq. 19 to obtain

$$\frac{1}{1 - m_o} = \left\{\frac{3m_s k_s}{HR\rho_p}\left(1 - \frac{Bi}{Bi + \phi_o\coth\phi_o - 1}\right)\right\}^{-1}\frac{Q}{V_L} + \frac{1}{1 - \exp(-K_L)} \quad (21)$$

The dimensionless group $K_L$ is independent of $Q$ since both $a_B$ and $V_B$ in Eq. 16 are proportional to $Q$. Hence, Eq. 21 shows that a plot of $(1 - m_o)^{-1}$ vs. $Q/V_L$, quantities which are known experimentally, should yield a straight line. The slope, along with the Biot number, $Bi$, and liquid-to-particle mass transfer coefficient, establish a relationship between $k_a/K$ and $k_r$ through Eq. 15. Also $K_L$, which is a function of the gas-to-liquid mass transfer coefficient $k_L a_B$, (Eq. 16), is obtainable from the intercept of such a plot.

Experimentally measured first moments include the residence time in the dead volume $V_d$ between the four-way valve and the dispersion tube (Figure 1) and between the upper surface of the slurry and the sample injection valve of the chromatograph. Thus the observed, reduced first moment $\mu_1^o$ can be expressed as

$$\mu_1^o = \frac{m_1}{m_o} + V_d/Q \quad (22)$$

Since $V_d = V_o - V_B V_L$, Eq. 10 for $m_1$ and Eq. 9 for $m_o$ can be used with Eqs. 11 and 20 to write Eq. 22 as

$$\mu_1^o\left(\frac{Q}{V_L}\right)m_o\left(\frac{K_L B_o}{1 - m_o}\right)^2 + V_B K_L B_o\left(\frac{2}{1 - \exp(-K_L)} - \frac{2}{K_L} - 1\right)$$
$$= \left(\frac{V_o}{V_L}\right)m_o\left(\frac{K_L B_o}{1 - m_o}\right)^2 + \frac{1}{H}\left[\frac{3m_s}{2}\left\{\frac{\beta}{\rho_p} + \frac{K}{[1 + k_r/(k_a/K)]^2}\right\}\right.$$
$$\left.\times\left\{\frac{\coth\phi_o - \phi_o\,\mathrm{csch}^2\phi_o}{\phi_o\left(1 + \dfrac{\phi_o\coth\phi_o - 1}{Bi}\right)^2}\right\} + \left(1 - \frac{m_s\beta}{\rho_p}\right)\right] \quad (23)$$

where $V_o$ is the dead volume without gas flow through the slurry. $V_o$ is related to known quantities by the expression:

$$V_T - V_L - V_{\text{carbon}} = V_o = V_T - V_L - \frac{m_s V_L(1 - \beta)}{\rho_p} \quad (24)$$

The second term on the left side of Eq. 23 is limited to $\pm V_B K_L B_o$. In our experiments this term is very small. This is because $H$ for oxygen is large and the residence of the gas bubbles is small so that $K_L$ from Eq. 16 becomes small. A straight line is expected if the left side of Eq. 23 is plotted vs. $m_o[K_L B_o/(1 - m_o)]^2$. The intercept of such a line yields a value of the ratio $k_r/(k_a/K)$, provided $K$ is known. The other quantities such as $K_L B_o$, and $\phi_o$ are known from the zero-moment results through Eq. 19. The slope of the line yields $V_o/V_L$. The resulting value can be checked by comparing it with $V_o$ estimated via Eq. 24.

In summary, from zero and first moment data, $k_s$, and $D_e$, Eqs. 21 and 23 can be used to obtain separate values of $k_a$ and $k_r$, provided $K$ is known.

### Evaluation of *K* from Oxygen Runs

When step functions of oxygen (10% $O_2$ and 90% He) are fed to the slurry, Eq. 10 reduces to

$$m_1 = \tau_g + \left(\frac{m_s K + 1}{H}\right)\frac{V_L}{Q} \qquad (25)$$

Including the residence time in the dead volume, the reduced first moment is

$$\mu_1^o = \left(\frac{m_s K + 1}{H} + \frac{V_o}{V_L}\right)\frac{V_L}{Q} \qquad (26)$$

Equation 26 shows that the slope of a plot of $\mu_1^o$ vs. $V_L/Q$ yields a value of $K$ provided that Henry's law constant for $O_2$ and $V_o$ are known. The zero moment for reversible adsorption is unity.

### Equations for Well-Mixed Gas Bubbles

Equations 1 and 2 are based upon plug flow of gas bubbles. At the other extreme, the residence time distribution of the bubbles would vary from zero to infinity with a distribution corresponding to that of fluid in a well-stirred vessel. For this case Eqs. 1 and 2 are replaced by

$$V_B V_L \frac{dC_g}{dt} = Q(C_{g_o} - C_g) - k_L a_B V_L\left(\frac{C_g}{H} - C_L\right) \qquad (27)$$

$$\left(1 - \frac{\beta_{ms}}{\rho_p}\right)\frac{dC_L}{dt} = k_L a_B\left(\frac{C_g}{H} - C_L\right) - k_s a_s[C_L - (C_i)_{r=R}] \qquad (28)$$

Solving Eqs. 27, 28, 3, and 4, with the boundary and initial conditions, leads to the following expressions for the moments:

$$m_o = \left(1 + K_L - \frac{K_L}{1 + B_o}\right)^{-1} \qquad (29)$$

$$m_1 = \frac{\tau_g(1 + B_o)^2 + K_L(B_s + \epsilon)}{(1 + B_o + K_L B_o)^2} \qquad (30)$$

As was done for the plug flow of gas bubbles, Eqs. 29 and 30 can be rearranged to suggest the proper functions for obtaining linear plots of the zero and first moment data. These forms, analogous to Eqs. 21 and 23, are

$$\frac{1}{1 - m_o} = \left[\frac{3m_s k_s}{HR\rho_p}\left(1 - \frac{Bi}{Bi + \phi_o \coth\phi_o - 1}\right)\right]^{-1}\frac{Q}{V_L} + \frac{1}{K_L} + 1 \qquad (31)$$

$$\left[\mu_1^o \frac{Q}{V_L} + V_B(1 - m_o)\right]\frac{m_o K_L^2}{(m_o + K_L m_o - 1)^2} = \frac{V_o m_o K_L^2}{V_L(m_o + K_L m_o - 1)^2} + \frac{1}{H}\left[\frac{3m_s}{2}\left\{\frac{\beta}{\rho_p} + \frac{K}{[1 + k_r/(k_a/K)]^2}\right\}\left\{\frac{\coth\phi_o - \phi\,\mathrm{csch}^2\phi_o}{\phi_o\left(1 + \frac{\phi_o \coth\phi_o - 1}{Bi}\right)^2}\right\} + \left(1 - \frac{m_s\beta}{\rho_p}\right)\right] \qquad (32)$$

Equations 21 and 23 for plug-flow bubbles and 31 and 32 for well-mixed bubbles differ only in their functions of $K_L$, the dimensionless group concerned with mass transfer from gas bubble to liquid (see Eq. 16). When $K_L$ approaches zero, which corresponds to our system of a slightly soluble gas ($H$ for oxygen is very large), the two sets of equations give the same values for the moments.

## EXPERIMENTAL RESULTS

Typical response curves for reaction conditions are shown in Figure 3. Data were measured for two different concentrations $m_s$ of carbon particles and at several gas flow rates for each $m_s$ (data for two flow rates are shown in Figure 3). After each series of runs at different flow rates, the slurry was discarded to avoid the buildup

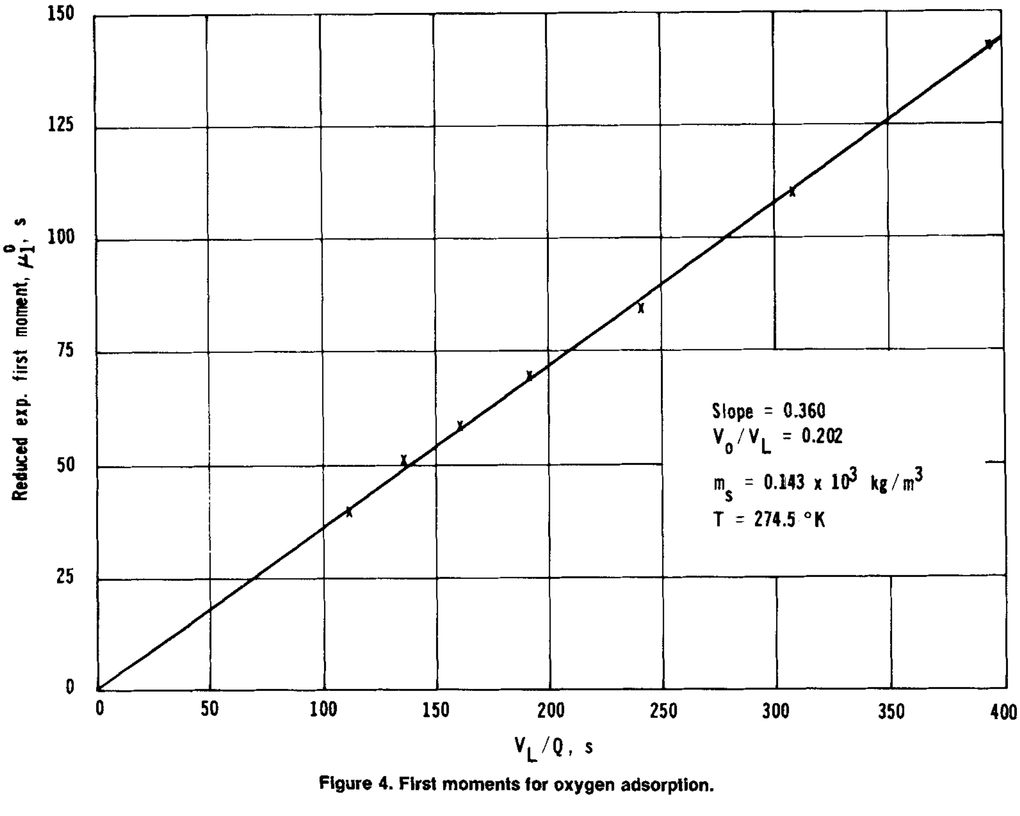

Figure 4. First moments for oxygen adsorption.

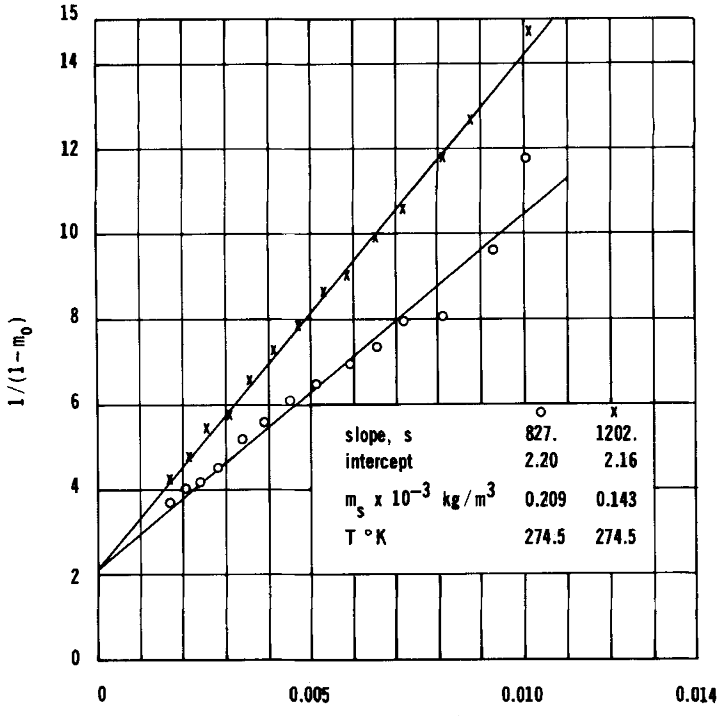

**Figure 5. Zero moments for reaction case.**

of sulfuric acid in the liquid. High $H_2SO_4$ concentrations have been found to reduce the reaction rate (Komiyama and Smith, 1975).

From such curves as those illustrated in Figure 3, the zero and first moments were calculated from Eq. 18. The advantage of obtaining data at many flow rates is that the linear plots referred to in the theory section give more accurate results than using single values of the moments in Eqs. 21 and 23. This procedure reduces the error that may be associated with one moment value. Also, Eq. 23 contains the first moment of the entire system. This avoids errors associated with independent determination of the dead volume.

### Adsorption Equilibrium Constant for Oxygen

Figure 4 shows first-order moments for oxygen alone (no reaction) plotted vs. $V_L/Q$, as suggested by Eq. 26. In the slurry used, the liquid volume was $1.04 \times 10^{-3}$ m$^3$ and the weight of carbon was 0.149 kg. The dead volume $V_o$ was estimated by subtracting the volume of the liquid and of the particles from the measured total volume of $1.32 \times 10^{-3}$ m$^3$. This value agreed well with that determined from plots of Eq. 23 using the reaction data. Thus, the estimated value of $V_o/V_L$ was 0.202, while the values determined from plots of Eq. 23 shown in Figure 6, were 0.226 for $m_s = 0.143 \times 10^3$ kg/m$^3$ and 0.207 for $m_s = 0.209 \times 10^3$ kg/m$^3$.

To obtain $K$ from the slope of the line in Figure 4, Henry's constant, $H$, for oxygen at 274.5 K was taken as 21.2 from the solubilities compiled by Linke (1965). Then from the slope and Eq. 26, $K = 16.4 \times 10^{-3}$ m$^3$/kg at 274.5 K. This result agrees, in general, with the measurements of Niiyama and Smith (1977 who obtained $K = 15.8 \times 10^{-3}$ m$^3$/kg at 278 K and $= 10.8 \times 10^{-3}$ m$^3$/kg at 299 K.

### Analysis of Moment Data for Reaction

The zero-moment values are plotted vs. $Q/V_L$ in Figure 5. The data points establish reasonably well-defined straight lines, as required by Eq. 21, although the scatter is greater at the higher gas flow rates. This is because at high flow rates the conversion is very low, and $m_o$ approaches unity. This means that $1 - m_o$, plotted in Figure 5, becomes less accurate. Nevertheless, the two lines for different $m_s$ values have nearly the same intercept, as suggested by Eq. 21. Linear regression was used to establish values of slope and intercept for all plots. The line for the larger $m_s$ has the smaller slope, also in agreement with Eq. 21. From the intercepts, $K_L$ is found to be nearly the same for the two $m_s$ runs: 0.606 and 0.621 for $m_s = 0.209$ and $0.143 \times 10^3$ kg/m$^3$, respectively. For the same reactor, impeller, and baffle geometry, the oxygen adsorption results of Niiyama and Smith (1977) correspond to $K_L = 0.68$ at 278 K.

Equations 19 and 21 show that the slope of the lines in Figure 5 can be used to calculate a value of $B_o$ for each gas flow rate, $Q$. These values are used in analyzing the first-moment data according to Eq. 23.

The quantity on the left side of Eq. 23, a modified first moment, when plotted vs. $m_o[K_L B_o/(1 - m_o)]^2$, a modified zero moment, should yield a straight line. Figure 6 is such a plot for the runs for the two $m_s$ values. According to Eq. 23, these two lines should be parallel with different intercepts. Actually, the lines cross, but the slopes are not greatly different (0.207 and 0.226). These slopes are equal to $V_o/V_L$ and their values agree well with the value obtained earlier in connection with the oxygen adsorption results.

The intercepts, 0.117 and 0.081, are functions of $k_r$ and $k_a/K$, as seen in in Eq. 23. These intercept values will be used in the next section, along with the zero moment results, to evaluate $k_a$ and $k_r$.

Recently, Chang and Smith (1983) considered the effect of the residence time of the gas bubbles on slurry reactor performance. Their results indicated that the effect was small for either slightly soluble or very soluble gases. We reanalyzed our zero-moment data according to Eq. 31, for a stirred-tank residence time distribution, and found $K_L$ to be 0.833 and 0.861 for $m_s = 0.209$ and $0.143 \times 10^3$ kg/m$^3$, respectively. These values differ somewhat, but not greatly, from the results of 0.606 and 0.621 for the plug-flow case (Eq. 21). When the first-moment results are plotted according to Eq. 32, the intercept values do not differ appreciably from those in Figure 6. This is shown in Figure 7. It is concluded that the residence-time distribution of the gas bubbles for our system had no effect on the adsorption and surface reaction rate constants, but did influence, somewhat, mass transfer from bubble to liquid.

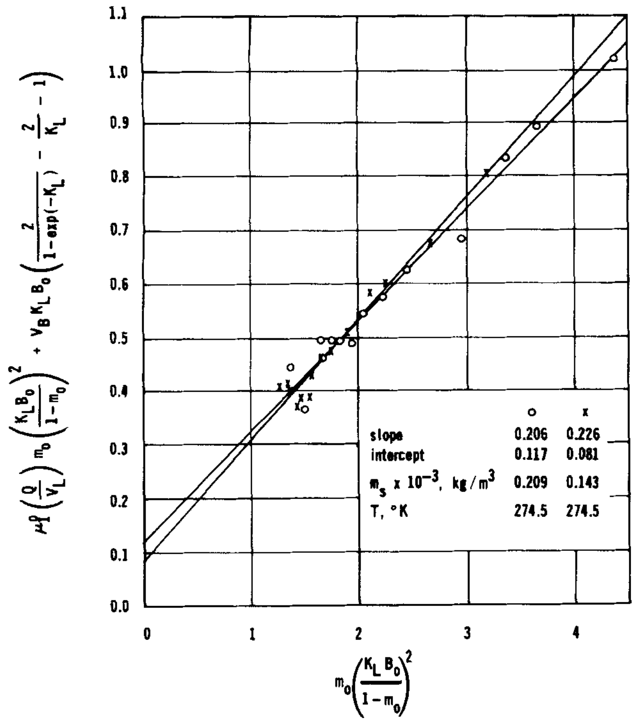

Figure 6. First moments for reaction case, plug-flow gas.

## DETERMINATION OF INDIVIDUAL RATE CONSTANTS

### Combined Rate-Constant Function from Zero Moment

Equation 21 shows that the slope of the zero-moment lines in Figure 5 is a function of liquid-to-particle mass transfer, $k_s$, and intraparticle diffusivity, $D_e$, through $\phi_0$ and $Bi$, as well as a function of the desired rate constants $k_a/K$ and $k_r$.

The experimental results for $k_s$ of Komiyama and Smith (1975) agreed with the correlation proposed by Furusawa and Smith (1973). Since the dimensions and geometry of our reactor, impeller, and baffles were the same, we used the correlation to determine a value of $k_s = 2.35 \times 10^{-4}$ m/s for our impeller speed and temperature. The diffusivity of oxygen in water at 298 K, $2.1 \times 10^{-9}$ m²/s, as given by Sherwood et al. (1975), was corrected to 274.5 K by the Stokes-Einstein equation and used in the correlation along with a value of $1.5 \times 10^{-7}$ kg·m/s for the viscosity of water.

Niiyama and Smith (1977) determined the effective diffusivity of oxygen in the pores of the same carbon to be $2.0 \times 10^{-9}$ m²/s, while Komiyama and Smith (1975) found $D_e = 5.3 \times 10^{-10}$ m²/s from their reaction data; both values were for 298 K. However, this uncertainty in $D_e$ does not appreciably affect the evaluation of $K_r$ and $k_a/K$. The nature of the function of the bracketed term in Eq. 21 is such that large changes in either $D_e$ or $k_s$ cause very little change in the function of $k_r$ and $k_a/K$ in brackets in Eq. 15. The insensitivity of $D_e$ is due to the small size of catalyst particles used in our work. The effectiveness factor is nearly unity. In this region the Thiele modulus, and therefore the effective diffusivity, can change greatly without changing the effectiveness factor significantly. For further calculations we used the result of Niiyama and Smith, corrected to 274.5 K, which gave $D_e = 1.14 \times 10^{-9}$ m²/s.

For the stated values for $k_s$ and $D_e$, the slopes of the lines in Figure 5 for the two $m_s$ values gave essentially the same result for the bracketed term in Eq. 15, that is, a combined rate constant of

$$\left[\frac{1}{K}\left(\frac{1}{k_a/K} + \frac{1}{k_r}\right)\right]^{-1} = 0.125 \times 10^{-3} \text{ m}^3/\text{kg carbon·s} \quad (34)$$

### Individual Rate Constants from First Moment

To evaluate the rate constant function in Eq. 23 from the intercepts in Figure 6, it is necessary to know the adsorption equilibrium constant $K$ for oxygen. A value of $16.4 \times 10^{-3}$ m³/kg at

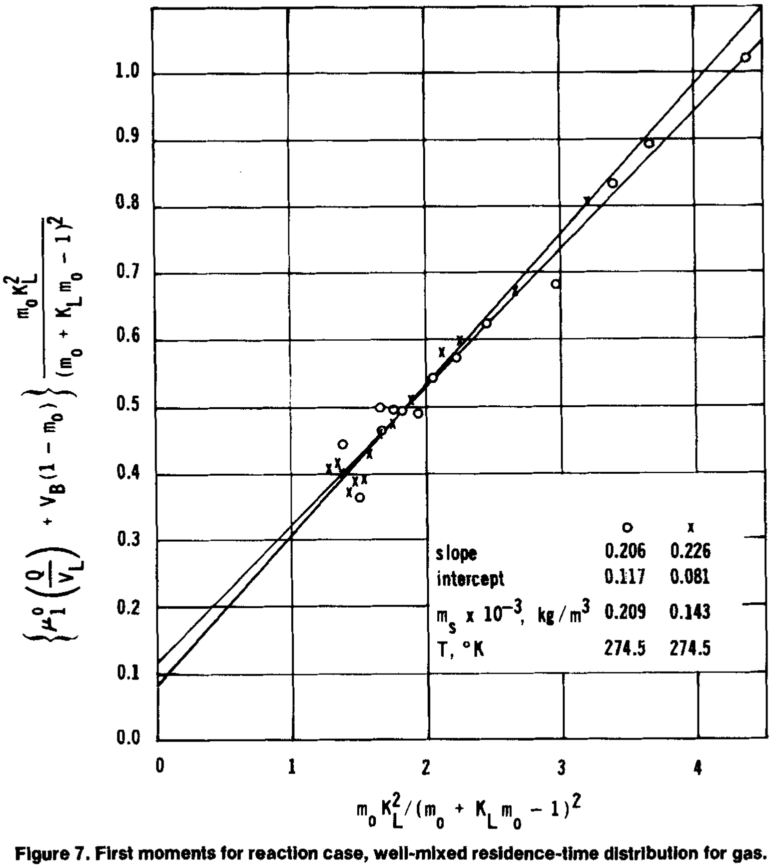

Figure 7. First moments for reaction case, well-mixed residence-time distribution for gas.

TABLE 3. ADSORPTION AND REACTION RATE CONSTANTS

| | | |
|---|---|---|
| $m_s$, kg/m$^3$ | $0.209 \times 10^3$ | $0.143 \times 10^3$ |
| Temp., K | 274.5 | 274.5 |
| $(1/k_a + 1/Kk_r)^{-1}$, m$^3$/kg·s | $0.125 \times 10^{-3}$ | $0.125 \times 10^{-3}$ |
| $k_r/(k_a/K)$ | 0.50 | 0.77 |
| $k_a$, m$^3$/kg·s | $0.38 \times 10^{-3}$ | $0.29 \times 10^{-3}$ |
| $k_r$, s$^{-1}$ | 0.011 | 0.014 |
| $K_L$ | 0.61 | 0.62 |

Parameter Values
$H = 21.2$
$K = 16.4 \times 10^{-3}$ m$^3$/kg
$k_s = 0.235 \times 10^{-3}$ m/s
$D_e = 1.14 \times 10^{-9}$ m$^2$/s

274.5 K was obtained from the oxygen adsorption data. However, it is uncertain whether this result is applicable when $SO_2$ and $H_2SO_4$ are present and there is competition for available sites on the carbon. From a general thermodynamic standpoint the chemical potential of adsorbed oxygen, for a given chemical potential in a gas, would be the same whether or not $SO_2$ and $H_2SO_4$ are present. However, the $K$ as we evaluate it is based upon concentrations rather than chemical potentials. Hence, the deviation of $K$ for reaction and nonreaction (solely $O_2$ adsorption) conditions depends upon deviations from ideal solutions in the gas, liquid, and solid phases. For low concentrations of oxygen in the liquid and on the carbon, the difference between the $K$ values could be small. The adsorption equilibrium constant under reaction conditions could, in principle, be determined by adding to the analysis the relationship, analogous to Eqs. 21 and 23, for the second moment. However, accurate second moments are difficult to obtain from experimental response curves because of the importance of the somewhat uncertain tail. Since our concentrations of oxygen in the liquid and on the carbon were very low, we have used $K = 16.4 \times 10^{-3}$ m$^3$/kg (on this point we are retaining one of the assumptions of the Hougen and Watson method). Then from Eq. 23, with $\phi_o$ known from the zero moment results, the ratio $k_r/(k_a/K)$ was found to be 0.497 for $m_s = 0.209 \times 10^3$ kg/m$^3$ and 0.772 for $m_s = 0.143 \times 10^3$ kg/m$^3$. With these numbers, the $k_a$ values for the two $m_s$ runs are 0.38 and $0.29 \times 10^{-3}$ m$^3$/kg·s, and the corresponding $k_r$ are 0.011 and 0.014 s$^{-1}$. These results are summarized in Table 3.

Niiyama and Smith (1977) in their nonreaction study with oxygen obtained $k_a = 0.32 \times 10^{-3}$ m$^3$/kg·s at the slightly higher temperature of 278 K. The agreement of this value with our results is very satisfactory since the data were obtained by different investigators, in the one case from adsorption-only experiments and in the other from reaction studies.

The value $k_r/(k_a/K)$ shown in Table 3 is particularly interesting in that it is equal to the ratio of reaction rate to desorption rate, as seen from Eq. 4. For example, the ratio of 0.50 for $m_s = 0.209 \times 10^3$ kg/m$^3$, suggests that for every three molecules of oxygen adsorbed, two are desorbed and one reacts to form $SO_3$. The values for this ratio, being neither very large or small, indicate that both adsorption and surface reaction affect the overall intrinsic rate. Thus for this case, it seems inappropriate to assume either adsorption or surface reaction to control the rate.

Komiyama and Smith (1975) from their steady state measurements could not separate $k_a$ and $k_r$. However, they suggested that adsorption of oxygen controlled the rate. This qualitative conclusion was based upon the observation that pretreatment of the slurry with high concentrations of oxygen enhanced the rate measured later at a lower concentration. From what is now known, this enhancement may have been due to a higher adsorbed oxygen concentration during the transient period.

## ACKNOWLEDGMENT

The discussions and assistance of Professor Francesc Recasens of the Polytechnic University of Barcelona, Spain, are gratefully acknowledged. Also, we appreciate the financial assistance of National Science Foundation Grant CPE-8026101.

## NOTATION

$a_B$ = surface area of gas bubbles per unit volume of bubble- and particle-free liquid, m$^2$/m$^3$
$a_s$ = surface area of catalyst particles per unit volume of bubble- and particle-free liquid, m$^2$/m$^3$
$Bi$ = Biot number, $Rk_s/D_e$
$B_o$ = dimensionless quantity defined by Eq. 14
$B_s$ = quantity defined by Eq. 11, s
$C_g$ = oxygen concentration in gas phase, kmol/m$^3$
$C_{g_o}$ = oxygen concentration in feed
$C_{g\infty}$ = oxygen equilibrium concentration in effluent gas
$C_i$ = oxygen concentration in liquid-filled pores of catalyst, kmol/m$^3$
$C_L$ = oxygen concentration in bulk liquid, kmol/m$^3$
$\overline{C}_g$ = Laplace transform of $C_g$, kmol·s/m$^3$
$D_e$ = effective diffusivity in the liquid-filled pores of catalyst particle, m$^2$/s
$H$ = Henry's constant for solubility of oxygen in water, $C_g/C_L$
$K$ = adsorption equilibrium constant for oxygen, m$^3$/kg
$k_a$ = adsorption rate constant, m$^3$/(kg)(s)
$k_L$ = gas bubble-to-liquid mass transfer coefficient, m/s
$K_L$ = dimensionless quantity defined by Eq. 16
$k_r$ = surface reaction rate constant, s$^{-1}$
$k_s$ = liquid-to-particle mass transfer coefficient, m/s
$L$ = depth of slurry, m
$m_o$ = zero moment
$m_1$ = first-order moment, s
$m_s$ = mass of catalyst particles per unit volume of bubble- and particle-free liquid, kg/m$^3$
$n$ = concentration of oxygen adsorbed on catalyst particles, kmol/kg carbon
$Q$ = volumetric gas flow rate, m$^3$/s
$r$ = radial distance from center of catalyst particle (spherical), m
$R$ = radius of catalyst particle, m
$s$ = Laplace variable, s$^{-1}$
$t$ = time, s
$v_B$ = vertical component of gas-bubble velocity, m/s
$V_B$ = bubble volume per unit volume of bubble- and particle-free liquid
$V_d$ = dead volume, including gas space over slurry, in tubing and trap (i.e., from four-way valve to sampling valve of chromatograph, Figure 1), m$^3$
$V_L$ = volume of liquid in the slurry, m$^3$
$V_o$ = dead volume with no gas flow, defined by Eq. 24, m$^3$
$V_T$ = volume of total system, including reactor, tubing, and trap, m$^3$
$z$ = vertical distance from bottom of slurry, m

### Greek Letters

$\beta$ = porosity of catalyst particle
$\epsilon$ = quantity defined by Eq. 12, s
$\mu_1^0$ = reduced first-order moment, including dead volume, defined by Eq. 26, s
$\phi_o$ = Thiele-type modulus defined by Eq. 15
$\rho_p$ = density of catalyst particle, kg/m$^3$
$\tau_g$ = residence time in gas phase, defined by Eq. 13, s

## LITERATURE CITED

Bennett, C. O., "A Dynamic Method for the Study of Heterogeneous Catalytic Reactions," *AIChE J.*, 13, 890 (1967).

———, "The Transient Method and Elementary Steps in Heterogeneous Catalysis," *Catal. Rev. Sci. & Eng.*, **13**, 2 (1976).

Chang, H., and J. M. Smith, "Effect of Residence Time Distribution of Gas Bubbles on Slurry Reactor Performance," *AIChE J.*, **29**, 699 (1983).

DeWaal, K. J. A., and J. C. Okeson, "The Oxidation of Aqueous Sodium Sulphite Solutions," *Chem. Eng. Sci.*, **21**, 559 (1966).

Furusawa, T., and J. M. Smith, "Fluid-Particle and Intraparticle Mass Transport Rates in Slurries," *Ind. Eng. Chem. Fund.*, **12**(2), 197 (1973).

Hinshelwood, C. N., *Kinetics of Chemical Change*, Ch. 8. Oxford U. Press, London (1940).

Hougen, O. A., and K. M. Watson, "Kinetics and Catalysis," *Chemical Process Principles*, 902, Wiley, New York (1947).

Kabel, R. L., and L. N. Johanson, "Reaction Kinetics and Adsorption Equilibria in the Vapor-Phase Dehydration of Ethanol," *AIChE J.*, 8(5), 621 (1962).

Kobayashi, M., and Kobayashi, H., "Application of Transient Response Method to the Study of Heterogeneous Catalysis, III," *J. Catal.*, **27**, 114 (1972).

Komiyama, H., and J. M. Smith, "Sulfur Dioxide Oxidation in Slurries of Activated Carbon," *AIChE J.*, **21**(4), 664 (1975).

Langmuir, I., "The Mechanism of the Catalytic Action of Platinum in the Reactions $2CO + O_2 = 2CO_2$ and $2H_2 + O_2 = 2H_2O$," *Trans. Fara. Soc.*, **17**, 621 (1921).

Linke, W. F., *Solubilities*, **II**, 1,228, Am. Chem. Soc., Washington, DC (1965).

Mattson, J. S., and H. B. Mark, Jr., *Activated Carbon*, 26, Marcel Dekker, New York (1971).

Niiyama, H., and J. M. Smith, "Adsorption of Nitric Oxide in Aqueous Slurries of Activated Carbon: Transport Rates by Moment Analysis of Dynamic Data," *AIChE J.*, **22**(6), 961 (1976).

Niiyama, H., and J. M. Smith, "Adsorption Rates of Oxygen in Aqueous Slurries of Activated Carbon," *AIChE J.*, **23**(4), 592 (1977).

Raghavan, N. S., and L. K. Doraiswamy, "On the Validity of Kinetic Modeling for Vapor-Phase Catalytic Reactions: Isomerization of *n*-Butene to Isobutene," *J. Catal.*, **48**, 21 (1977).

Ramachandran, P. A., and J. M. Smith, "Dynamics of Three-Phase Slurry Reactors," *Chem. Eng. Sci.*, **32**, 873 (1977).

Sherwood, T. K., R. L. Pigford, and C. R. Wilke, *Mass Transfer*, 26, McGraw-Hill, New York (1975).

Smith, J. M., "35 Years of Applied Catalytic Kinetics," *Ind. Eng. Chem. Fund.*, **21**, 327 (1982).

Suzuki, M., and J. M. Smith, "Kinetic Studies by Chromatography," *Chem. Eng. Sci.*, **26**, 221 (1971).

Weng, H.-S., and J. M. Smith, "Mass Transfer, Adsorption, and Reaction in Slurry Reactors," *J. Chem. Eng.*, **28**, 115 (1984).

Weller, S., "Kinetic Models in Heterogeneous Catalysis," *Adv. in Chem. Ser.*, **148**, 156 (1975).

*Manuscript received Sept. 2, 1983; revision received Feb. 28, 1984, and accepted Mar. 1.*